

LA-UR-17-22766 (Accepted Manuscript)

Synthesis and characterization of surrogate nuclear explosion debris: urban glass matrix

Campbell, Keri
Judge, Elizabeth
Dirmyer, Matthew R.
Kelly, Daniel
Czerwinski, Ken R.

Provided by the author(s) and the Los Alamos National Laboratory (2017-12-08).

To be published in: Journal of Radioanalytical and Nuclear Chemistry

DOI to publisher's version: 10.1007/s10967-017-5367-y

Permalink to record: <http://permalink.lanl.gov/object/view?what=info:lanl-repo/lareport/LA-UR-17-22766>

Disclaimer:

Approved for public release. Los Alamos National Laboratory, an affirmative action/equal opportunity employer, is operated by the Los Alamos National Security, LLC for the National Nuclear Security Administration of the U.S. Department of Energy under contract DE-AC52-06NA25396. Los Alamos National Laboratory strongly supports academic freedom and a researcher's right to publish; as an institution, however, the Laboratory does not endorse the viewpoint of a publication or guarantee its technical correctness.

1

Title page

2 Names of the authors: Keri Campbell¹, Elizabeth J. Judge¹, Matthew R. Dirmyer¹, Dan
3 Kelly¹, Ken Czerwinski²

4 Title: Synthesis and Characterization of Surrogate Nuclear Explosion Debris: Urban
5 Glass Matrix

6 Affiliation(s) and address(es) of the author(s):

7 ¹ Chemical Diagnostics and Engineering
8 Chemistry Division, C-CDE
9 Los Alamos National Laboratory
10 P.O. Box 1663, MS J964
11 Los Alamos, New Mexico 87545
12 ²Department of Chemistry
13 Radiochemistry Program
14 University of Nevada, Las Vegas
15 4505 Maryland Parkway, Box 454003
16 Las Vegas, Nevada 89154-4003

17

18 E-mail address of the corresponding author:

19 kcampbell@lanl.gov

20

21 **Synthesis and Characterization of Surrogate Nuclear**
22 **Explosion Debris: Urban Glass Matrix**

23 Keri Campbell¹, Elizabeth J. Judge¹, Matthew R. Dirmyer¹, Dan Kelly¹, Ken Czerwinski²

24 ¹*Chemical Diagnostics and Engineering, Chemistry Division C-CDE, Los Alamos*
25 *National Laboratory, P.O. Box 1663, MS J964, 87545, Los Alamos, NM, USA*

26 ²*Department of Chemistry, Radiochemistry Program, University of Nevada Las Vegas,*
27 *4505 S. Maryland Pkwy box 454003, 89154, Las Vegas, NV, USA*

28 **Abstract**

29 Surrogate nuclear explosive debris was synthesized and characterized for major, minor,
30 and trace elemental composition as well as uranium isotopics. The samples consisted of
31 an urban glass matrix, equal masses soda lime and cement, doped with 500 ppm uranium
32 with varying enrichments. The surface and cross section morphology were measured with
33 SEM, and the major elemental composition was determined by XPS. LA-ICP-MS was
34 used to measure the uranium isotopic abundance comparing spot, line scans, and depth
35 profiling sampling techniques. A fraction of each sample was leached and solution ICP-
36 MS was performed to compare accuracy and precision of isotopic measurements to LA-
37 ICP-MS results. The results provide an example of the application and utility of LA-ICP-
38 MS for forensics applications.

39 **Keywords**

40 Surrogate Nuclear Explosive Debris, Uranium, Urban Matrix, Isotope Ratio, Fallout

41 **Introduction**

42 Post-detonation nuclear forensics uses the physio-chemical processes associated with a
43 nuclear detonation to identify the device type and the source of the nuclear material in the
44 device [1]. After a nuclear detonation, several key questions need to be answered to
45 provide the decision makers with the necessary information to protect and serve the
46 community at risk. The Joint Working Group of the American Physical Society and the
47 American Association for the Advancement of Science have detailed a general timeline
48 of the pertinent questions that need to be answered [2]. The yield of the detonation,
49 general sophistication of the device, whether the device was primarily uranium or
50 plutonium, and isotopic composition of fuel components all factor in to provenance
51 determination and device design reconstruction.

52 During a nuclear detonation, the weapon and environment surrounding the detonation are
53 melted and vaporized [3]. Surface detonations melt environmental material that can then
54 either remain in place or be incorporated into the nuclear fireball. As the fireball cools,
55 the device debris and environmental material are mixed into fused glassy material known
56 as nuclear explosive melt debris [4]. There are two main types of nuclear explosive melt
57 debris: ground glass and aerodynamic fallout [5]. The nuclear explosive melt debris is
58 mainly composed of the displaced environment, and the device debris is present only in
59 trace quantities [1]. For this reason, it is important to understand the local environment in
60 the case of an urban detonation. The major components of buildings in cities are glass,
61 steel and concrete. Glass and steel elemental compositions are fairly consistent in
62 construction materials. Concrete consists of many components depending on the desired
63 properties, where the elemental composition can vary significantly. Nominally, concrete
64 contains cement, chemical admixtures and aggregates [6]. The cement and aggregates
65 contain trace elements that may interfere with post-detonation nuclear forensics.

66 The formation of surrogate nuclear explosive debris (SNED) is of interest to the nuclear
67 forensic community for training, method development of analytical techniques, and
68 measurement exercises. The SNED material allows for laboratories to practice efficiency
69 of answering relevant questions in a post-detonation scenario since nuclear explosive
70 melt debris is limited in quantity and accessibility. The shortage of nuclear explosive
71 melt debris is due to the fact that testing was suspended in agreement with the

72 Comprehensive Nuclear-Test-Ban Treaty. In recent years, a variety of approaches to
73 synthesize SNED materials have been published [7-11]. Each technique attempts to
74 replicate and answer different characteristics of complex, inhomogenous nuclear
75 explosive melt debris. The heat sources range from high power lasers [7, 8], electric arc
76 [9], to furnaces [10, 11] in attempts to fuse the materials to mimic either the ground glass
77 or aerodynamic fallout physical and chemical characteristics. The chemical matrices used
78 in SNED range from NIST certified reference standards [7], borosilicate glass doped with
79 highly enriched uranium (HEU) [11], to 50:50 combination of cement and soda lime
80 doped with Xe [8]. In this work, SNED samples were prepared using soda lime and
81 Portland cement to mimic an urban detonation. The SNED material is then doped with
82 different enrichments of uranium to determine if the matrix would interfere with uranium
83 isotopic analysis, and what elements can be expected to remain in nuclear explosive melt
84 debris after an urban detonation.

85 The International Atomic Energy Agency (IAEA) has listed common analytical
86 techniques used in nuclear forensic analysis [12]. These techniques are categorized based
87 on elemental and isotopic bulk analysis, imaging, and microanalysis. Most of the
88 techniques listed for elemental and isotopic analysis require lengthy digestion and
89 separations prior to analysis, this sample preparation leads to a delay in the key questions
90 needed to be answered following a post-detonation scenario [12]. Laser ablation
91 inductively coupled plasma-mass spectrometry (LA-ICP-MS) as a nuclear forensic
92 technique would minimize the number of steps in the handling process, maximizing
93 throughput and turn-around time relative to current non-destructive assay techniques with
94 the ability to determine isotopic composition and concentrations of elements of interest in
95 nuclear explosive debris. LA-ICP-MS has the ability to measure bulk or local analysis
96 with high spatial resolution of trace and isotopic analysis depending on the sampling
97 technique (ie: spot, line scan, and depth profiling). The second portion of this work
98 compares the different laser ablation sampling techniques to solution ICP-MS analysis to
99 determine the viability of using LA-ICP-MS in a post-detonation scenario on a complex
100 matrix.

101 **Experimental**

102 *Sample Preparation*

103 The main components of the urban glass matrix SNED samples were modeled after the
104 World Trade Center debris, which composed of glass and concrete from the buildings [7].
105 Therefore, the SNED samples prepared consisted of a 50:50 mixture of soda lime and
106 cement. The soda lime was purchased from Sigma-Aldrich and contained 75.2% SiO₂,
107 11.2% CaCO₃, 13.7% Na₂CO₃. The cement was purchased from Quikrete and contains
108 Portland cement, silica sand, lime, limestone, iron oxide pigment and clay. The SNED
109 samples were doped with 500 ppm of U₃O₈ with ²³⁵U isotope concentrations of 0.72
110 (natural), 20, 50, and 80% ²³⁵U. The 20 and 80% enriched ²³⁵U₃O₈ materials were
111 purchased from New Brunswick Laboratory as NBL CRM standards. The 50% enriched
112 U₃O₈ material was prepared in the laboratory, as described in the supplemental section.
113 The total mixture of 50:50 soda lime:cement and the U₃O₈ powder was vortexed for 1
114 minute, then placed in a 5% Rh:Pt or 5% Au:Pt crucible. The samples were then heated
115 under argon atmosphere at 1500 °C for 1 hour. The theoretical concentration of uranium
116 in the melt glass was found to be 506.1 ± 43.3 ppm, determined by the amount added to
117 the powder mixture prior to heating. A second set of doped uranium glass samples were
118 prepared by Lawrence Livermore National Laboratory (LLNL) [13]. These samples were
119 used as standards to quantify the amount of uranium in the blank SNED sample. The
120 samples were doped with 5, 50, and 500 ppm natural uranium.

121 *Scanning Electron Microscope/Energy Dispersive X-ray Emission Spectroscopy*

122 Analysis of the surface and cross section morphology of the SNED samples was
123 performed using a Scanning Electron Microscope (SEM). The JEOL JSM-6360LV SEM
124 was equipped with a secondary electron and backscatter electron detectors. The natural
125 uranium SNED sample was broken into pieces and mounted on copper tape. After
126 mounting, the sample was sputter coated with palladium gold alloy to avoid charging on
127 the surface, since the sample is non-conductive. The samples included a cross section,
128 top, and bottom portion of the material. The images were collected using secondary
129 electron imaging mode with an accelerating voltage of 20 kV and a working distance of

130 11 mm. The SEM also has the capability to measure elemental analysis through energy
131 dispersive x-ray emission spectroscopy (EDS) using INCA mapping software. The
132 elemental mapping was used to correlate the XPS data collected. For the EDS analysis, x-
133 ray energies of 0 to 10 keV were detected.

134 *X-ray Photoelectron Spectroscopy*

135 X-ray photoelectron spectroscopy (XPS) analysis was used to determine the bulk
136 elements in the urban matrix glass materials. XPS data was collected using a Physical
137 Electronics VersaProbe II system with a base pressure below 1×10^{-7} Pa. A variable-size,
138 monochromated Al K_{α} x-ray source (1487 eV) was used throughout, and photoelectrons
139 were energy sorted using a hemispherical analyzer. The XPS spectra are reported in terms
140 of binding energy (BE) and instrument calibration was performed in accordance with
141 ASTM procedure. Elemental composition was determined using survey scans at a pass
142 energy of 117 eV. A pass energy of 29 eV was used for high-resolution scans to
143 determine chemical valence state. Depth profiling was carried out using 2 kV argon ions.
144 Charge neutralization for insulating samples is accomplished by focusing low energy ions
145 and electrons at the spot of x-ray impingement. The blank SNED sample was crushed
146 into two pieces and mounted on carbon tape. The samples were sputtered for 10 minutes
147 prior to analysis to exclude any surface contamination. This sputtering time is estimated
148 to drill several hundred angstroms into the sample.

149 *Laser Ablation-Inductively Coupled Plasma-Mass Spectrometry*

150 Analysis was conducted using LA-ICP-MS to determine the isotope ratio of the uranium
151 and the trace constituents of the SNED samples. The laser ablation was an Electro
152 Scientific Industries (ESI) New Wave Research (NWR) 213 Laser Ablation system
153 equipped with a Nd:YAG deep UV (213 nm) laser was used for the analysis. The NWR
154 213 was coupled to a Thermo Scientific iCAP Q ICP-MS. Helium carrier gas was used to
155 deliver the ablated material to the ICP-MS at a flow rate of 1 Lmin^{-1} . Prior to analysis
156 ICP-MS parameters were optimized using NIST 612 glass. Three different sampling
157 techniques were performed in order to characterize the material for homogeneity. The
158 first analysis determined uranium isotopic homogeneity of the surface using laser

159 sampling of four randomly chosen areas of the sample with stationary laser spots. The
 160 second analysis, depth profile, verified uranium isotopic homogeneity of the samples in
 161 regards to depth. The depth profile analysis was conducted by drilling down into the
 162 sample with sequential laser shots, decreasing in spot size from 110 μm to 40 μm in
 163 increments of 10 μm for a total of 8 samplings per area. This procedure was repeated for
 164 a total of three times per sample for standard deviation calculations. The third laser
 165 sampling technique used line scan analysis, where the scan speed of the laser was set at 5
 166 μmsec^{-1} . Mass scan surveys were conducted on the 20% enriched $^{235}\text{U}_3\text{O}_8$ SNED sample
 167 to qualitatively determine trace elements in the matrix. Line scan analysis was used as the
 168 sampling technique in the mass scan surveys and the quantification of uranium in the
 169 blank SNED sample. The laser fluence, repetition rate and plasma power were held
 170 constant for all sampling techniques at 2 Jcm^{-2} , 20 Hz, and 1550 W. The parameters that
 171 varied for each type of analysis are listed in Table 1. The samples were probed for the
 172 isotopic abundance of ^{234}U , ^{235}U , ^{236}U , and ^{238}U . The dwell time of the ICP-MS using in
 173 laser ablation mode was 50 ms for all isotopes evaluated.

174 **Table 1** Instrument parameters for solid (LA-ICP-MS) and solution (ICP-MS) analysis

Instrument Parameters	Mass Scan Survey LA-ICP-MS	Quantification LA-ICP-MS	Depth Profile LA-ICP-MS	Spot Analysis LA-ICP-MS	Line Scan LA-ICP-MS	Solution ICP-MS
Spot size (μm)	85	85	varied	85	85	n/a
Duration of ablation (s)	90	30	5	5	30	n/a
Dwell time (ms)	50	50	50	50	50	varied
Ar Nebulizer gas flow (Lmin^{-1})	0.613	0.5193	0.635	0.586	0.596	0.9093
Integration time (s)	n/a	30	20	20	30	n/a
Sample size (n)	3	3	24	4	3	5

175

176 To compare the accuracy and precision of laser ablation to solution phase analysis, a
 177 portion of the SNED samples were gently crushed for leaching experiments. The small
 178 fractions of the crushed SNED samples, (masses listed in Table 2) were placed in 0.5 mL

179 of leaching solution containing ultra pure concentrated acids (0.1 mL concentrated HF
180 and 0.4 mL 70% HNO₃). The leaching time was 15 hours for the natural, 20, 50, and 80%
181 ²³⁵U₃O₈ samples, and 72 hours for the blank SNED sample. This variation is due to the
182 overall concentration of uranium in the samples. The concentration of uranium in the
183 blank SNED sample was significantly less than the other samples, as indicated by the
184 uranium signal intensity obtained during LA-ICP-MS analysis. The blank SNED sample
185 solution used in ICP-MS analysis used all of the leaching solution (0.5 mL) diluted with
186 30 mL of 2% HNO₃. A stock solution was made for the remaining samples using 50 µL
187 of the leaching solution in 10 mL of 2% HNO₃. The stock solution was then diluted by a
188 factor of 18 for ICP-MS analysis. For the solution analysis of the leached SNED samples,
189 the ICP-MS parameters were optimized using Thermo Scientific Set Up solution. The
190 dwell times were varied depending on the abundance of the isotope. If the isotope
191 abundance was below 50% the dwell time was 100 ms, if the abundance was ≥ 50% the
192 dwell time was 50 ms.

193 **Table 2** Amount of SNED samples used in leaching study for solution isotopic analysis

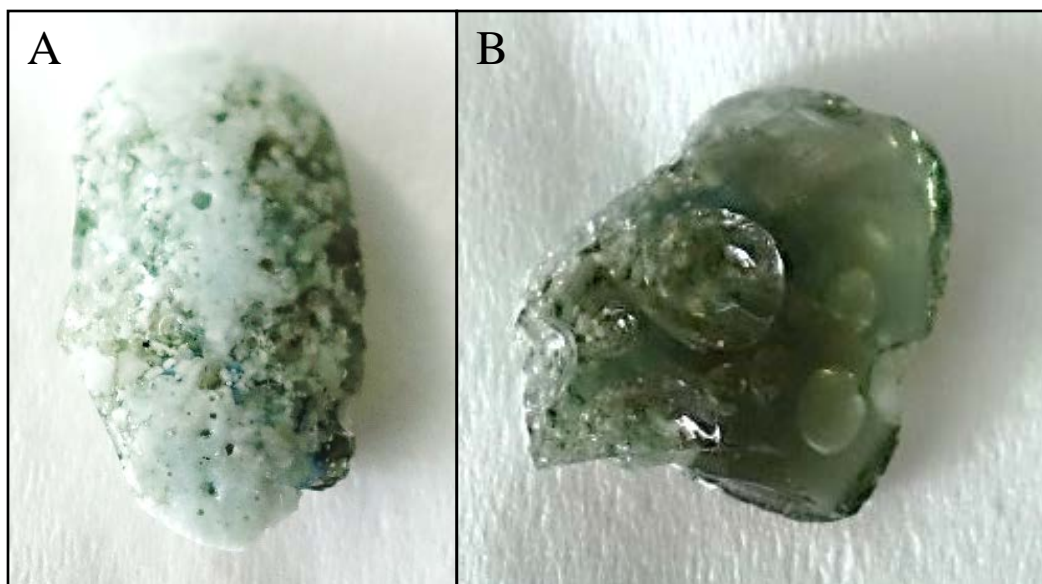
Sample Name	Mass (mg)
Blank	32.5
Natural	13.7
20% U ²³⁵	11.6
50% U ²³⁵	7.9
80% U ²³⁵	6.3

194 **Results and discussion**

195 *Synthesis of Material*

196 Nuclear explosive melt debris from near-surface and underground detonations include
197 diverse mixtures of glass, silicates, and subordinate oxides [5, 14-16]. The homogeneity
198 of the melt glass after detonation ranges from glassy spheroidal aerodynamic fallout to
199 ground glass which forms a smooth glassy surface transitioning to compositional
200 variations of unmelted soil [5, 17]. Each sample of the SNED material was observed to
201 have a white crystalline top (Figure 1 A) and greenish-blue transparent glass bottom with

202 inclusions of black (Figure 1 B), consistent with phases observed in ground glass samples
203 of trinitite [18, 19]. The phase separation is either metal loading of the starting material,
204 where two different liquid phases are more stable than one single phase during the
205 melting process or incomplete melting of the starting material. However, the short melt
206 time of one hour was successful in producing the desired heterogenous sample.

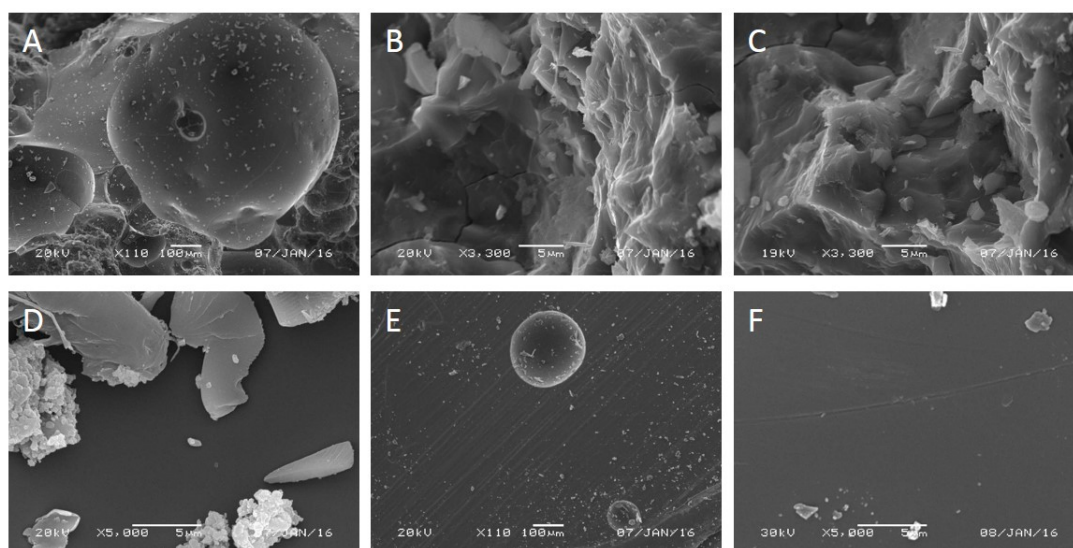


207

208 **Fig. 1** Photos of SNED samples; A) White phase on top of samples, B) Greenish-blue
209 phase on bottom of samples

210 The surface and cross section morphology of the SNED material was investigated using
211 SEM. One of the natural uranium SNED fragments was mounted on its side to view a
212 cross section of the glass shown in Figure 3 A-C. Vesicles, cracks, and pits were
213 observed in the cross section as well as the surface of the green phase of the sample
214 (Figure 3 E). The presence of internal cavities and pores are also observed in ground
215 glass trinitite [19]. Conglomerates were visible on the surface of the white phase, shown
216 in Figure 3 D. It is unclear if the conglomerates are a precipitate phase from the melting
217 process, or if this phase is from incomplete melting of the starting material at various
218 stages. The green phase was smooth (Figure 3 F) with surface bubbles (Figure 3 E) as
219 previously mentioned. The vesicles and bubbles are due to volatile and low-boiling point
220 elements being trapped in the melt during the cooling process. The morphology of the
221 SNED samples are consistent with observations made with ground glass [19, 20] from the

222 Trinity test. The geometry of the furnace used in the melting process did not allow for
223 quenching, which did not seem to affect the desired morphology of the SNED samples.



224

225 **Fig. 2** SEM images of natural uranium SNED sample: A-C) Cross section images
226 highlighting the internal cavities and pores, D) Surface image showing aggregates
227 composing of the white top phase, E) Surface images of the bottom greenish-blue phase
228 with surface bubble, and F) Smooth surface image of the bottom greenish-blue phase.

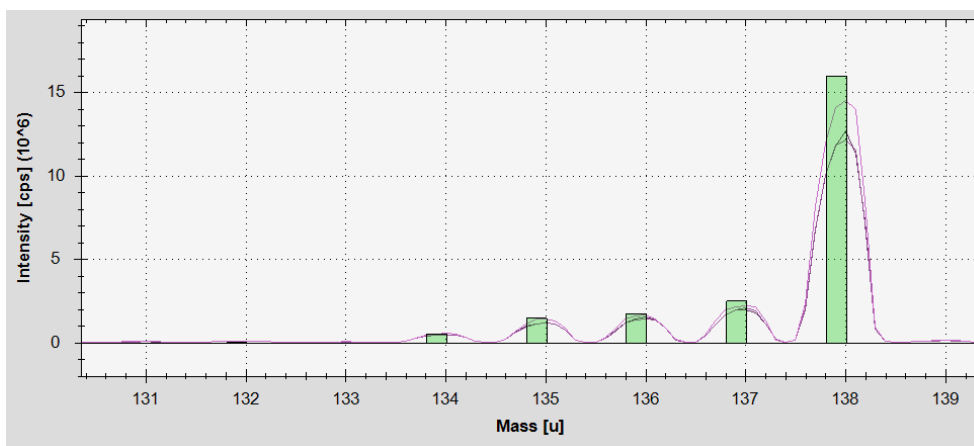
229 To determine the bulk elements of the white and green phases of the SNED samples, the
230 blank SNED sample was analyzed using XPS. The limit of detection of XPS is assumed
231 to be ≥ 0.1 atomic percent (at. %). The results of the XPS analysis are listed in Table 3,
232 and were corroborated with EDS measurements. All of the elements detected in this
233 analysis are assumed to be in their oxide form, and correlate with analysis performed on
234 trinitite, with the exception of carbon [14, 21]. The temperatures of an actual nuclear
235 detonation would result in carbon volatilizing within the cloud. The mass of the samples
236 were measured before and after heating, where the average mass loss was found to be
237 12.9 ± 2.7 %. This mass loss is due to volatile and low-boiling point elements
238 incorporated into the cement and soda lime raw material volatilizing during the melting
239 process. Comparing the green phase of the melt glass to the white phase, overall the
240 major elements are homogeneous with the exception of carbon and aluminum. There is
241 significantly more carbon in the white phase and twice the amount of aluminum in the
242 green phase than the white phase. The color of the white phase would indicate a

243 carbonate (either sodium or calcium) rather than elemental carbon. Calcium is a main
244 component in the soda lime used in the synthesis and also present in Portland cement
245 from the lime and limestone constituents. The remaining major elements, aluminum,
246 magnesium, and iron are from the Portland cement used in the synthesis. Iron is
247 incorporated into the cement via iron oxide pigment, where the aluminum is a main
248 component of clay minerals. Magnesium is abundant in the earth's crust, therefore it
249 could be incorporated into any of the constituents comprising the cement.

250 **Table 3** Elemental composition (at. %) of the green and white phases of blank SNED
251 sample

Element	Atomic Concentration (at. %)	
	White Phase	Green Phase
C 1s	7.89	1.01
O 1s	55.66	59.81
Na 1s	3.86	2.81
Mg 2p	0.53	0.53
Al 2p	1.65	3.32
Si 2p	25.56	25.48
Ca 2p	4.68	6.7
Fe 2p _{3/2}	0.16	0.34

252 To determine any trace constituents that may be an issue during nuclear forensic
253 measurements of post detonation debris containing cement, a mass scan survey was
254 performed using LA-ICP-MS. Three line scans from different areas of the 20% enriched
255 ²³⁵U SNED sample were investigated. Line scan ablations of the sample were 90 seconds
256 in duration at 5 μsec^{-1} , with the instrument parameters listed in Table 1. A mass scan
257 survey was collected from m/z 7-238. Comparing the natural abundance of each isotope
258 with the signal intensity of the ICP-MS, element identification can be deduced. An
259 example of this technique is shown in Figure 3 for barium. This technique was used to
260 identify several elements found in the matrix but is more difficult for elements with only
261 one isotope.



262

263 **Fig. 3** Example of survey scan isotope fingerprint for barium, with the relative isotope
 264 abundance shown as green bars and the spectral data shown as the three red curves.

265 The minor and trace elements detected using LA-ICP-MS were a mixture of intermediate
 266 and refractory elements found in melt glass [22]. The signal intensities at the m/z
 267 measured are consisted with ppb to low ppm levels. Depending on the type of aggregate
 268 or binder used to make cement, trace and bulk elements will vary. Elements were
 269 identified to be equally distributed between the green and white phase include titanium,
 270 chromium, manganese, nickel, rhenium, and uranium . The well mixing of uranium in the
 271 SNED material is consistent with core samples analysis of underground nuclear explosive
 272 debris [14]. Table 4 lists the identified elements that were not homogenous between the
 273 green and white phases of the material. Since there are no standards for the trace elements
 274 for this matrix, a relative ratio of the signal intensities is reported. Rubidium, strontium,
 275 zirconium, and molybdenum lie in areas of interest in the thermal fission yield curve.
 276 Prior knowledge of materials may not be known in a post detonation scenario, resulting
 277 in a possible inaccurate nuclear forensic evaluation of the aftermath. For this reason, it is
 278 necessary to be able to accurately measure the isotope abundance of the fuel, for example
 279 uranium or plutonium, within the matrix. Polyatomic interferences such as PtAr, and
 280 PbO₂ can influence ²³⁵U weight percent measurements [23, 24]. A significant amount of
 281 lead was detected in the green glass phase which could lead to inaccurate measurements
 282 of uranium isotopic ratios. Due to the possibility of lead and platinum incorporation in a
 283 post-detonation scenario in an urban environment, survey scans of the melt glass would
 284 be essential in determining interferences and areas of interest to accurately measure the

285 isotope abundance of the fuel used in the device for LA-ICP-MS analysis. The use of a
286 collision cell would also mitigate polyatomic interferences.

287 **Table 4** Ratio of the signal intensities of trace elements detected in 20% ²³⁵U SNED
288 sample results from LA-ICP-MS analysis

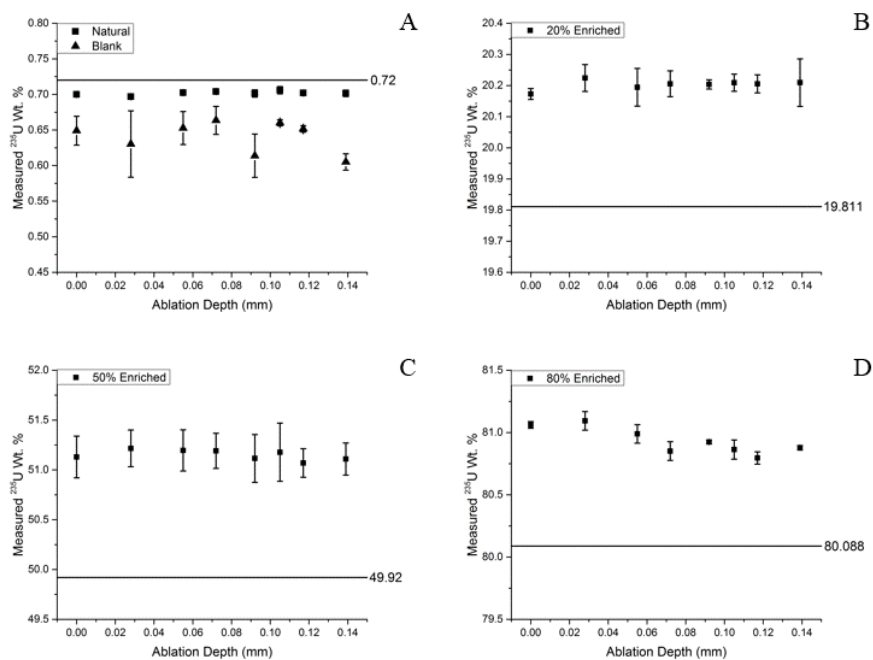
Element	Cu	Zn	Rb	Sr	Zr	Mo	Ba	Ce	W	Pb
Green/White	0.090	2.481	1.551	1.458	0.606	0.066	2.480	1.646	0.186	5.524
Std. Dev.	0.002	0.790	0.168	0.093	0.080	0.008	0.104	0.217	0.026	0.590

289 *Uranium Isotopic Ratio Measurements using LA-ICP-MS*

290 Laser ablation ICP-MS analysis has been used in literature to evaluate SNED and trinitite
291 extensively, [8, 18, 21, 25-28] but is not listed as an analytical tool for nuclear forensics
292 by the IAEA [12]. However, the IAEA includes ICP-MS as an analytical tool for nuclear
293 forensics to determine isotopic and elemental concentrations in samples. A side by side
294 comparison of the uranium isotope measurements was performed with LA-ICP-MS and
295 ICP-MS on the SNED samples to determine the viability of using LA-ICP-MS in a post-
296 detonation scenario. The same ICP-MS was used for both sample introduction methods,
297 keeping the detector variability constant and comparing sample introductory techniques.
298 The laser ablation sampling techniques include spot, line scan, and depth profile analysis.
299 Each sampling technique evaluated the white side of the material to avoid polyatomic
300 interferences from PbO₂ abundance in the green phase, detected during the mass scan
301 survey. These techniques are looked at to determine if the small sampling area is
302 representative of the bulk material, but also highlight the spatial resolution of laser
303 ablation.

304 The depth profile sampling method was performed using LA-ICP-MS to determine the
305 homogeneity of the uranium isotope ratio within the sample. The method drilled down
306 into the sample with sequential laser shots, decreasing in spot size from 110 μm to 40 μm
307 in increments of 10 μm. The variation in spot size was designed to ensure that the laser-
308 sample coupling was consistently at the bottom of the crater, rather than the sides of the
309 crater, due to re-solidification during the ablation process. The depth measurements
310 reported in Figure 4 are estimated from a separate experiment where the laser was
311 focused within the crater between samplings. The average depth of sampling was found

312 to be $18.6 \pm 0.7 \mu\text{m}$ for a total change in depth of $139.0 \pm 4.2 \mu\text{m}$. The isotopic
 313 measurements from the focusing study were found to be the same as the measurements
 314 without refocusing indicating that focusing the laser between measurements is not needed
 315 for this system. The distance between measurements most likely falls within the depth of
 316 focus in regards to the beam waist of the laser. In the graphs shown in Figure 4, the
 317 horizontal line denotes the theoretical value for each sample. Overall the samples appear
 318 to be homogenous with depth as shown, and the blank SNED sample has the most
 319 variability of the isotope ratio measurements with regards to depth. The high standard
 320 deviation for the drill down method analysis of the blank sample can be explained by the
 321 surface morphology, and due to the stationary nature of the sampling method. If the area
 322 chosen is next to a pit/void in the sample the laser contact with the surface is
 323 compromised, where the laser energy is not uniformly absorbed by the surface.



324 **Fig. 4** LA-ICP-MS depth analysis of the SNED samples at varying enrichments. A)
 325 Blank and natural, B) 20% enriched ^{235}U , C) 50% enriched ^{235}U and D) 80% enriched
 326 ^{235}U
 327

328 The analysis of the blank SNED sample revealed a higher than expected abundance of
 329 uranium. These samples were prepared to simulate environmental samples and are
 330 therefore accurate in terms of the blank containing some level of uranium. The source of

331 the uranium detected in the blank sample is most likely from the aggregates used in the
332 concrete material, where the concentration of uranium can vary significantly depending
333 on the ore body. In order to quantify the amount of uranium in the blank, the second set
334 of uranium doped glass samples prepared by LLNL were used as standards for LA-ICP-
335 MS analysis. The linear correlation value (R^2) for both the ^{235}U and ^{238}U calibration
336 curves were found to be 0.999. When quantifying uranium using LA-ICP-MS, it is
337 important to use standards that have relatively the same isotopic abundances of ^{235}U and
338 ^{238}U . Although the calibration curves are isotope specific, they determine the overall
339 elemental concentration. The total concentration of uranium in the blank sample was
340 found to be 3.68 ± 0.12 ppm and 3.42 ± 0.09 ppm for ^{235}U and ^{238}U calibration curves,
341 respectively. The variation in the quantification measurement between ^{235}U and ^{238}U is
342 most likely due to the lower isotopic ratio of the blank sample (0.66) in relation to the
343 standards (0.72) used to make the measurement. This will result in an artificial increase
344 of the ^{235}U concentration and decrease of the ^{238}U concentration as shown in the
345 measurement. The actual uranium concentration in the sample is likely to be some value
346 between 3.42 ± 0.09 ppm and 3.68 ± 0.12 ppm.

347 Each sampling technique is evaluated for accuracy and precision by calculating the
348 percent bias and the percent relative standard deviation (RSD), respectively. The results
349 of the accuracy and precision of the measurements are listed in Table 5. Corrections for
350 mixing of two different uranium sources has been described elsewhere, [5, 18] so it will
351 not be addressed in this analysis. Therefore, the relative accuracy of the measurement is
352 compared for the sampling methods. The blank and natural SNED samples measured
353 values are significantly lower than the expected theoretical value for all of the sampling
354 techniques tested, with the highest percent bias values calculated for the sample series.
355 Since the sources of uranium used in the blank and natural samples are not certified
356 material, the assumption that they are purely natural may not be true. For the enriched
357 samples, the depth profile sampling method has the highest deviation from the certified
358 values, in regards to the accuracy of the isotopic ratio measurement. The measured values
359 for the enriched samples of all the sampling methods, except the line scan analysis, are
360 greater than the theoretical values. The line scan LA-ICP-MS sampling method percent
361 bias values are within statistical error of the solution phase ICP-MS analysis. This

362 suggests that the line scan analysis sampling method is just as accurate as solution phase
 363 ICP-MS analysis for determining the bulk isotopic ratio of the material without needing
 364 to digest the sample.

365 The precision of each sampling method is evaluated by comparing the percent RSD
 366 values. The sampling method that resulted in the most precise measurement of the blank
 367 and natural isotope ratios was the LA-ICP-MS line scan analysis. The precision of all the
 368 sampling methods for the enriched samples fall below 0.5 % RSD, where the depth
 369 profile sampling method is the most consistent of solid sampling methods for the
 370 enriched samples. The performance of each solid sampling technique in regards to
 371 precision of the measurement will depend on the surface morphology and geometry of
 372 the sample. It is recommended that an optimization of the sampling technique be
 373 performed for each type of sample (soil, glass, etc.) when using LA-ICP-MS as a nuclear
 374 forensic analytical tool.

375 **Table 5** Solid (LA-ICP-MS) and solution phase (ICP-MS) analysis of the SNED samples
 376 at varying enrichments of uranium

Theoretical ²³⁵U Wt. %	Sampling Technique	Measured ²³⁵U Wt. %	% Bias	Wt. % Std. Dev.	Wt. % RSD
0.72 (Blank)	Line Scan	0.635	-11.8	0.002	0.26
	Spot	0.685	-4.8	0.015	2.20
	Depth Profile	0.641	-11.0	0.022	3.40
	Solution	0.668	-7.3	0.003	0.41
0.72 (Natural)	Line Scan	0.689	-4.3	0.001	0.18
	Spot	0.685	-4.8	0.002	0.31
	Depth Profile	0.702	-2.5	0.003	0.38
	Solution	0.685	-4.8	0.002	0.26
19.811	Line Scan	19.702	-0.6	0.014	0.07
	Spot	20.047	1.2	0.049	0.25
	Depth Profile	20.203	2.0	0.015	0.07
	Solution	20.008	1.0	0.010	0.05
49.92	Line Scan	49.635	-0.6	0.131	0.26
	Spot	50.413	1.0	0.018	0.04
	Depth Profile	51.150	2.5	0.052	0.10
	Solution	50.213	0.6	0.018	0.04

80.088	Line Scan	79.922	-0.2	0.171	0.21
	Spot	80.916	1.0	0.033	0.04
	Depth Profile	80.932	1.1	0.106	0.13
	Solution	80.247	0.2	0.008	0.01

377

378 **Conclusions**

379 The synthesis of SNED samples was successful in producing samples that were similar to
380 ground glass trinitite in both chemical heterogeneity and morphology characteristics. The
381 melting temperature and profile resulted in a two phase glass that had vesicles, cracks,
382 and pits. The urban matrix was shown to be complex resulting in minor and trace
383 elements that can obscure nuclear forensic calculations necessary to answer key questions
384 including yield, sophistication of the device, and provenance of materials. Lead was also
385 detected in significant quantities that could affect uranium isotope measurements using
386 ICP-MS or LA-ICP-MS without sample treatment, due to polyatomic interferences of
387 PbO₂. Polyatomic interferences can be limited with the use of an ICP-MS that contains a
388 collision cell. Samples with complex spatial and chemical heterogeneity such as these
389 would be beneficial to the nuclear forensics community for measurement exercises,
390 training, and method development of analytical techniques.

391 This work also explored the use of LA-ICP-MS for quantitative isotopic analysis of
392 uranium, concentration of uranium, and qualitative determination of minor and trace
393 constituents found in the SNED samples. The soda lime and cement uranium SNED
394 samples isotopic composition was analyzed by LA-ICP-MS and compared with the
395 leached analysis using solution phase ICP-MS. Within the solid sample analysis, LA-
396 ICP-MS, the samples were investigated for homogeneity using line scan, depth profile
397 and spot laser sampling. The samples were found to be homogeneous with regards to
398 surface and depth analysis of uranium concentration and isotope ratios. All of the
399 sampling techniques including solution analysis of the leached glass measured values for
400 the blank and natural samples are significantly lower than the expected theoretical. Since
401 the sources of uranium used in these samples are not certified material, the assumption

402 that they are purely natural may not be true. Thermal Ionization Mass Spectrometry
403 measurements of the uranium isotopes would be needed to verify the theoretical values
404 assumed in this work are correct. The results for each LA-ICP-MS sampling method
405 compared very well with solution phase ICP-MS. This demonstrates that LA-ICP-MS is a
406 rapid technique for post-detonation analysis with percent bias within statistical error of
407 solution analysis and reasonable precision. Using LA-ICP-MS in a post-detonation
408 scenario is beneficial in providing answers to key questions in a more timely fashion than
409 solution phase ICP-MS.

410 **Acknowledgements**

411 This material is based upon work supported by the Department of Energy National
412 Nuclear Security Administration under Award Number: DE-NA0000979 through the
413 Nuclear Science and Security Consortium, and [NA-241 info](#).

414 The author's would like to thank Kim Knight and colleagues at Lawrence Livermore
415 National Laboratory for preparing the second set of uranium glass samples used for
416 quantification in this study.

417 This report was prepared as an account of work sponsored by an agency of the United
418 States Government. Neither the United States Government nor any agency thereof, nor
419 any of their employees, makes any warranty, express or limited, or assumes any legal
420 liability or responsibility for the accuracy, completeness, or usefulness of any
421 information, apparatus, product, or process disclosed, or represents that its use would
422 not infringe privately owned rights. Reference herein to any specific commercial
423 product, process, or service by trade name, trademark, manufacturer, or otherwise does
424 not necessarily constitute or imply its endorsement, recommendation, or favoring by
425 the United States Government or any agency thereof. The views and opinions of
426 authors expressed herein do not necessarily state or reflect those of the United States
427 Government or any agency thereof.

428 **References**

- 429 1. Moody KJ, Hutcheon ID, Grant PM (2005) Nuclear Forensic Analysis, CRC
430 Press, Boca Raton, FL
- 431 2. APS and AAAS (2008) Nuclear Forensics: Role, State of the Art, Program Needs,
432 Printed in the United States of America ISBN 978-0-87168-722-7
- 433 3. Glasstone S, Dolan PJ (1977) The Effects of Nuclear Weapons, 3rd Ed. United
434 States Department of Defense and the Energy Research and Development
435 Administration
- 436 4. Miller CF (1964) Biological and Radiological Effects of Fallout from Nuclear
437 Explosions, Office of Civil Defense Department of Defense, Washington D.C.
- 438 5. Lewis LA, Knight KB, Matzel JE, Prussin SG, Zimmer MM, Kinman WS,
439 Ryerson FJ, Hutcheon ID (2015) Spatially-resolved analyses of aerodynamic
440 fallout from a uranium-fueled nuclear test. *J. Environmental Radioactivity*
441 148:183-195
- 442 6. Hewlett PC (1998) *Lea's Chemistry of Cement and Concrete*, 4th edn. Elsevier
443 Ltd, Oxford
- 444 7. Liezers M, Fahey AJ, Carman AJ, Eiden GC (2015) The formation of trinitite-like
445 surrogate nuclear explosion debris (SNED) and extreme thermal fractionation of
446 SRM-612 glass induced by high power CW CO₂ laser irradiation. *J Radioanal*
447 *Nucl Chem* 304:705-715
- 448 8. Liezers M, Carman AJ, Eiden GC (2016) The preparation of non-radioactive
449 glassy surrogate nuclear explosion debris (SNED) loaded with isotopically altered
450 Xe. *J Radioanal Nucl Chem* 307:1811-1817
- 451 9. Dai ZR, Crowhurst JC, Grant CD, Knight KB, Tang V, Chernov AA, Cook EG,
452 Lotscher JP, Hutcheon ID (2013) Exploring high temperature phenomena related

- 453 to post-detonation using an electric arc. *J Appl Phys* 114:204901.
454 doi:10.1063/1.4829660
- 455 10. Harvey SD, Liezers M, Antolick KC, Garcia BJ, Sweet LE, Carman AJ, Eiden
456 GC (2013) Porous chromatographic materials as substrates for preparing synthetic
457 nuclear explosion debris particles. *J Radioanal Nucl Chem* 298:1885-1898
- 458 11. Carney KP, Finch MR, McGrath CA, Martin LR, Lewis RR (2014) The
459 development of radioactive glass surrogates for fallout debris. *J Radioanal Nucl*
460 *Chem* 299:363-372
- 461 12. IAEA (2006) Nuclear Forensics Support Reference Manual, IAEA Nuclear
462 Security Series No. 2 Technical Guidance, IAEA, Vienna
- 463 13. Eppich GR, Wimpenny JB, Leever ME, Knight KB, Hutcheon ID, Ryerson ID
464 (2016) Characterization of low concentration uranium glass working materials.
465 Lawrence Livermore National Laboratory LLNL-TR-645481.
- 466 14. Smith DK (1995) Characterization of Nuclear Explosive Melt Debris.
467 *Radiochimica Acta* 69:157-167
- 468 15. Fahey AJ, Zeissler CJ, Newbury DE, Davis J, Lindstrom RM (2010)
469 Postdetonation nuclear debris for attribution. *PNAS* 107(47):20207-20212
- 470 16. Eppich GR, Knight KB, Jacob-Hood TW, Spriggs GD, Hutcheon ID (2014)
471 Constraints on fallout melt glass formation from a near-surface nuclear test. *J*
472 *Radioanal Nucl Chem* 302:593-609
- 473 17. Eby N, Hermes R, Charnley N, Smoliga JA (2010) Trinitite-the atomic rock.
474 *Geology Today* 26(5):180-185
- 475 18. Bellucci JJ, Simonetti A, Koeman EC, Wallace C, Burns PC (2014) A detailed
476 geochemical investigation of post-nuclear detonation trinitite glass at high spatial
477 resolution: Delineating anthropogenic vs. Natural components. *Chemical Geology*
478 365: 69–86.

- 479 19. Belloni F, Himbert J, Marzocchi O, Romanello V (2011) Investigating
480 incorporation and distribution of radionuclides in trinitite. *J Environmental*
481 *Radioactivity* 102:852-862
- 482 20. Hermes RE, Strickfaden WB (2005) A new look at trinitite. *J Nucl Weapons* 2:2-
483 7
- 484 21. Sharp N, McDonough WF, Ticknor BW, Ash RD, Piccoli PM, Borg DT (2014)
485 Rapid analysis of trinitite with nuclear forensic applications for post-detonation
486 material analyses. *J Radioanal Nucl Chem* 302:57-67
- 487 22. Izrael YA (2002) *Radioactive fallout after nuclear explosions and accidents.*
488 Elsevier, Saint Louis
- 489 23. Pollington AD, Kinman WS, Hanson SK, Steiner RE (2016) Polyatomic
490 interferences on high precision uranium isotope ratio measurements by MC-ICP-
491 MS: applications to environmental sampling for nuclear safeguards. *J Radioanal*
492 *Nucl Chem* 307:2109-2115
- 493 24. Campbell K, Unger A, Kerlin W, Hartmann T, Bertoia J, Judge E, Dirmyer M,
494 Czerwinski K (2016) Limiting spectroscopic interferences of ^{239}Pu and ^{237}Np in a
495 UO_2 matrix using LA-ICP-MS. *J Radioanal Nucl Chem* 310:533-540
- 496 25. Wallace C, Bellucci JJ, Simonetti A, Hainley T, Koeman EC, Burns PC (2013) A
497 multi-method approach for determination of radionuclide distribution in trinitite. *J*
498 *Radioanal Nucl Chem* 298:993-1003
- 499 26. Donohue PH, Simonetti A, Koeman EC, Mana S, Burns PC (2015) Nuclear
500 forensic applications involving high spatial resolution analysis of Trinitite cross-
501 sections. *J Radioanal Nucl Chem* 306:457-467
- 502 27. Bellucci JJ, Simonetti A, Wallace C, Koeman EC, Burns PC (2013) Lead Isotopic
503 Composition of Trinitite Melt Glass: Evidence for the Presence of Canadian
504 Industrial Lead in the First Atomic Weapon Test. *Anal Chem* 85:7588-7593

505 28. Bellucci JJ, Simonetti A, Wallace C, Koeman EC, Burns PC (2013) Isotopic
506 Fingerprinting of the World's First Nuclear Device Using Post-Detonation
507 Materials. *Anal Chem* 85:4195-4198.

508 Supplemental

509 Two sources of 20% and 80% enriched $^{235}\text{U}_3\text{O}_8$ were down-blended to produce a third
510 source of 50% enriched $^{235}\text{U}_3\text{O}_8$. The desired masses of the two enrichments, (50.8 mg of
511 20% $^{235}\text{U}_3\text{O}_8$, and 50.7 mg of 80% $^{235}\text{U}_3\text{O}_8$), were added to 10 mL of ultra-pure
512 concentrated nitric acid from JT Baker to dissolve the oxides. The solution was then
513 heated to 100 °C for 15 minutes and then cooled to room temperature for 1.5 hours. De-
514 ionized water (15 mL) was added to the solution, followed by 20 mL of concentrated
515 ammonium hydroxide saturated in oxalate. The container was then placed in an ice bath
516 for 10 minutes as the reaction is exothermic. The solution was then vortexed for 2
517 minutes followed by centrifugation at 2500 rpm for 5 minutes. The solution was then
518 decanted and the precipitate was freeze dried overnight. The precipitate was then calcined
519 at 200 °C for 2 hours, 500 °C for 2 hours, and 600 °C for 12 hours in ambient air to
520 produce 50% enriched $^{235}\text{U}_3\text{O}_8$. Powder x-ray diffraction was performed on the sample
521 for phase identification and confirmed the 50% enriched $^{235}\text{U}_3\text{O}_8$ was $\alpha\text{-U}_3\text{O}_8$.